Reprinted from ENGINEERING FOR POWER, *Vol. 102, No. 4, October, 1980*

D. J. Salamone
Project Engineer,
Compressor Division,
Allis-Chalmers Corporation,
Milwaukee, Wisc.
Assoc. Mem. ASME

E. J. Gunter
Professor,
Dept. of Mechanical and Aerospace Engineering,
University of Virginia,
Charlottesville, Va.
Mem. ASME

Synchronous Unbalance Response of an Overhung Rotor with Disk Skew

This paper deals with the influence of disk skew on the synchronous unbalance response of flexible rotors in damped bearings. A simple overhung rotor is treated to illustrate the effects of various combinations of unbalance and disk skew on the amplitude and phase angle response at the disk and bearings. The paper shows that it is impossible to balance the rotor at all speeds by single plane balancing even if three correction planes are employed. The presence of disk skew may be best detected by monitoring the far bearing for a rapid phase angle decrease after passing through the first critical speed.

Introduction

Within the past ten years, the technology for the design of high-speed turbo-rotors has become very sophisticated. These advanced design capabilities have supported the continuing emphasis in industry to build rotating machinery with larger capacities. Larger capacity designs often require longer, more flexible rotors capable of operating above several critical speeds. In order to safely operate through these critical speeds, a good balance is necessary to control rotor amplitudes and bearing forces.

Many extensive multi-plane balancing techniques, based on the influence coefficient method, have been developed in this country. These techniques have assumed that (1) the transverse axes of the rotor disks are perpendicular to the elastic centerline of the shaft, and (2) the shaft is not distorted. With these assumptions, the synchronous rotor excitation is due only to asymmetric radial mass distributions or disk eccentricities. However, in an actual rotor the shaft centerline may be bowed and the disks can be skewed, which induces effective external forces and moments on the shaft. A rotor might appear to be well balanced at a particular design speed when balanced with a technique that considers only the radial unbalance forcing function. However, the rotor may be considerably out of balance at other operating speeds as a result of the shaft bow and disk skew effects. These influences can induce large amplitudes of motion on the rotor when it is operating in the vicinity of critical speeds. Ultimately, these large amplitudes can lead to extensive rotor and bearing damage.

Extensive publications are available on the dynamic unbalance response of complex flexible rotor systems by such authors as Lund and Orcutt [1], Kawamo, et al. [2], Kirk and Gunter [3], Wolfe and Wong [4], Barrett, et al. [5], and Koenig [6]. However, their investigations have focused primarily on rotor response due to the action of radial unbalance forces, but do not include shaft bow and disk skew. Kikuchi [7] made a significant contribution toward developing the matrix transfer equations for a multimass rotor with shaft bow and disk skew. However, his formulation has several discrepancies which are pointed out in [8]. Nicholas, et al. [9] presented a very complete treatment of the influence of shaft bow on the single mass rotor in rigid bearings.

The incorporation of disk skew is considerably more complicated than the treatment of the radial unbalance alone. In order to examine the influence of disk skew, two additional equations of motion must be considered to represent the disk angular motion and gyroscopic moments. When the general Euler rotation angles are implemented to develop the dynamic equations of motion for a general precessing, nutating gyroscope, these equations are highly nonlinear. Consequently, only limited solutions can be obtained analytically. For example, Lund's [10] original synchronous unbalance response equations include the non-linear gyroscopic terms for a disk (however, permanent disk skew is not considered). This treatment requires an iterative procedure to include these nonlinear effects. Yamamoto [11] presented the general equations of motion for a skewed disk, transformed into linearized stationary coordinates. The Yamamoto approach employed the transformation of the Eulerian equations to a fixed coordinate system. Then, the governing dynamic equations of motion are obtained by applying a disk kinetic energy expression to Lagrange's equations of motion. The resulting equations are then linearized for small displacements and rotations. In the treatment of rotating machinery, the disk angular displacements and the shaft slopes are small in comparison to the characteristic length of the rotor. Therefore, the Yamamoto formulation may be used to describe the disk linear dynamic equations of motion.

The case of a single, overhung skewed disk on a uniform elastic shaft was treated by Benson [12] at the University of Virginia. Benson demonstrated that permanent disk skew can have a pronounced effect on the dynamics of the rotor shaft and that the single plane balancing procedure is not adequate to balance the overhung skewed disk at all speeds. This analytical formulation is of considerable value as it provides insight into the dynamic behavior of an overhung rotor system. However, this procedure is not readily adaptable to the evaluation of a multimass stepped rotor with skewed disks.

Salamone and Gunter [13] presented the governing transfer matrix equations to include the effects of disk skew and shaft bow, in addition to unbalance, for a general multimass rotor in fluid film bearings. The importance of these two additional effects was illustrated in an analysis of a multimass water pump. It was reported that bow and

Contributed by the Gas Turbine Division of The American Society of Mechanical Engineers and presented at the Gas Turbine Conference and Exhibit and Solar Energy Conference, San Diego, California, March 12–15, 1979. Manuscript received at ASME Headquarters December 26, 1978. Paper No. 79-GT-135.

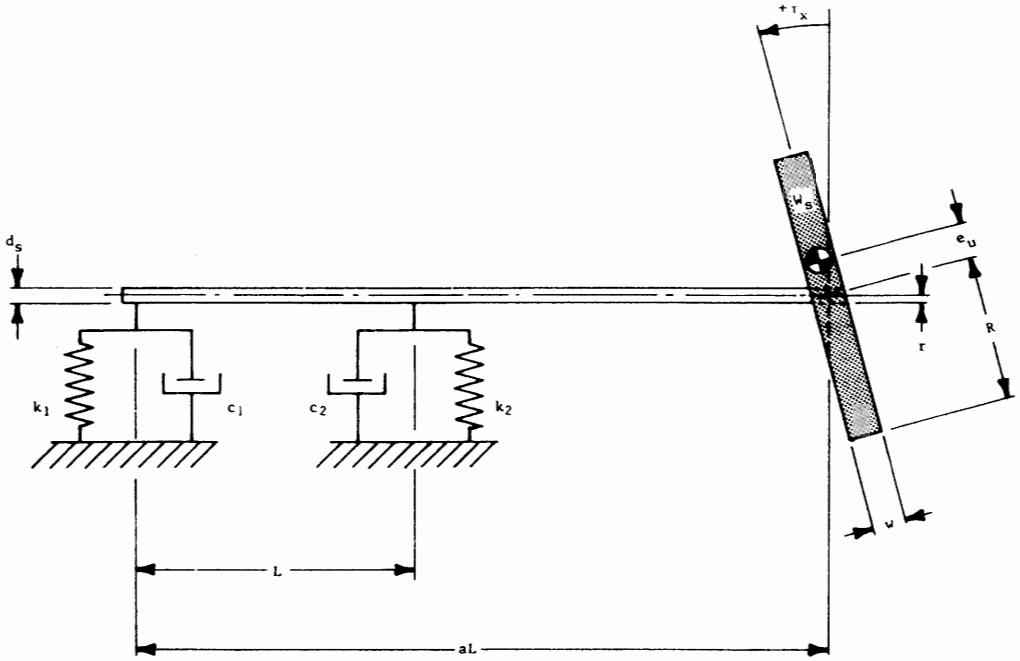

Fig. 1 Single mass unbalanced rotor with overhung skewed disk on flexible damped bearings

Table 1 Rotor Model Parameters*

L = 255.25 cm (100.49 in.)	R = 50.8 cm (20.0 in.)	I_p = 4.082 × 10^6 N-cm^2 (1.4224 × 10^5 lbf-in^2)
aL = 340.33 cm (133.99 in.)	r = 5.08 cm (2.0 in.)	I_t = 2.039 × 10^6 N-cm^2 (7.106 × 10^4 lbf-in^2)
d_s = 10.16 cm (4.0 in.)	w = 5.08 cm (2.0 in.)	$k_1 = k_2$ = 13171.11 N/cm (7520.9 lbf/in.)
W_s = 3132.04 N (704.14 lbf)	e_u = 0.025 cm (10 mils)	$c_1 = c_2$ = 51.28 N-s/cm (29.28 lbf-s/in.)
τ_x = 0.0684°	U_x = 8114.53 gm-cm (112.66 oz-in)	

* Refer to Fig. 1

skew can significantly alter the rotor response due to unbalance; particularly at the critical speeds.

Another formulation which has been successfully used to express the dynamical equations of motion of a complex rotor bearing system is the modal representation of Childs [14]. In the Childs derivation, the products of inertia have also been included, although the effects of disk skew and products of inertia were not explored.

In the treatment of disk skew in this paper, the angle of the disk skew τ is considered to be very small. Under these circumstances, it can be shown that the product of interia term is proportional to the product of the difference between the polar and transverse moments of inertia and the skew angle. An effect equivalent to disk skew can be generated by two radial out of phase unbalance components, which are separated by a finite axial distance on the disk. The resulting system is mathematically identical to a small disk skew, and the resulting unbalance components produce a bending moment about the disk center.

The results of [13] have inspired further study of disk skew effects to better understand the fundamental rotor behavior and the impact on balancing. Because of the complexity of the multimass rotor behavior with shaft bow and disk skew, it is desirable to first examine a single mass overhung rotor on flexible damped bearings with a skewed disk. The cases presented herein illustrate the potential impact of disk skew in comparison to, and in combination with, the commonly treated unbalance excitation.

Dynamic Motion of the Overhung Thin Disk Rotor

Description of the Rotor System. The single-mass overhung rotor model, as shown in Fig. 1, is a dimensionalized version of the model analyzed by Benson [12]. This model was used for verification of the general multimass matrix transfer equations in [8] and [13]. It should be noted that this is strictly an arbitrary rotor configuration which has been selected to illustrate the effects of disk skew on the synchronous rotor response. The dimensional characteristics of the thin disk rotor system are given in Table 1. Note that the bearing coefficients are assumed constant with rotor speed. The values of stiffness and damping were calculated from the nondimensional expressions in [12]. Bearing cross-coupling and shaft weight are neglected.

Nomenclature

A = amplitude ratio, δ/e_u
e_u = radial unbalance mass eccentricity, L
f = frequency ratio, ω/ω_{cr}
I_p = polar mass moment of inertia of disk, FLT^2
I_t = transverse mass moment of inertia of disk, FLT^2
$j = \sqrt{-1}$
K = constant
K_{ij} = stiffness, FL^{-1}
m = disk mass, FT^2L^{-1}
m_j = mass at station j, FT^2L^{-1}
t = time, T
U = complex unbalance, $U_x + jU_y$, FL
w = disk thickness, L
z = complex rotor displacement, L
α_j = angular location of unbalance at station j, RAD
β_j = angular location of disk skew at station j, RAD
δ = rotor displacement, L
θ = complex rotor slope, RAD
τ = complex disk skew angle, $\tau_x + j\tau_y$, RAD
ω = angular rotor shaft rotational speed, T^{-1}
ω_{cr} = angular rotor critical speed, T^{-1}

For a "thin" disk, the polar moment of inertia I_p is greater than the transverse moment of inertia I_t. In this analysis, it is assumed that the polar is twice the transverse. Note that this system will have only one synchronous critical speed of forward precession. The Benson analysis also considered the thick disk configuration in which the transverse moment of inertia I_t is greater than the polar moment of inertia I_p. In that case, there are two critical speeds of forward synchronous precession.

Rotor Equations of Motion. The general transfer matrix equations used in this analysis have previously been derived and presented in [8] and [13], respectively. These multimass matrix equations become greatly simplified for the single mass overhung rotor illustrated in Fig. 1. Benson [12] expressed eight equations of motion that specifically apply to this rotor system, with isotropic bearings and a massless shaft. These eight equations were expressed as the following four complex equations:

$$e^{j\omega t}\begin{Bmatrix} me_u\omega^2 e^{j\alpha} \\ \tau\omega^2(I_p - I_t)e^{j\beta} \\ 0 \\ 0 \end{Bmatrix} = \begin{bmatrix} m & 0 & 0 & 0 \\ 0 & I_t & 0 & 0 \\ 0 & 0 & 0 & 0 \\ 0 & 0 & 0 & 0 \end{bmatrix}\begin{Bmatrix} \ddot{Z} \\ \ddot{\theta} \\ \ddot{Z}_1 \\ \ddot{Z}_2 \end{Bmatrix} + \begin{bmatrix} C & 0 & 0 & 0 \\ 0 & -j\omega I_p & 0 & 0 \\ 0 & 0 & C_1 & 0 \\ 0 & 0 & 0 & C_2 \end{bmatrix}\begin{Bmatrix} \dot{Z} \\ \dot{\theta} \\ \dot{Z}_1 \\ \dot{Z}_2 \end{Bmatrix} + \begin{bmatrix} K_{zz} & K_{z\theta} & K_{z1} & K_{z2} \\ & K_{\theta\theta} & K_{\theta_1} & K_{\theta_2} \\ (\text{SYM}) & & K_{11} & K_{12} \\ & & & K_{22} \end{bmatrix}\begin{Bmatrix} Z \\ \theta \\ Z_1 \\ Z_2 \end{Bmatrix} \quad (1)$$

Examination of these equations of motion illustrate several important features. First, it is observed that there are two forcing functions acting on the disk deflection equation Z and slope equation θ which are generated by radial unbalance and disk skew. The second feature, observed from the moment forcing term, is that the sign of the term is dependent upon whether the polar moment of inertia is larger than the transverse moment of inertia. In the case of a thick disk, where the transverse is larger than the polar, the skew gyroscopic moment would be opposite in sign compared to the moment for a thin disk. Therefore, considerably different dynamic effects are observed with disk skews on thick disks as compared to thin disks. This feature will be discussed in detail in a future paper.

Synchronous Response of the Overhung Thin Disk Rotor. The rotor response results for five computer cases are illustrated in Figs. 2–7. These are plots of the dimensionless amplitude and phase angle versus frequency ratio for the three rotor locations corresponding to the near bearing (closest to disk), the far bearing and the disk. The amplitude of motion δ is made dimensionless by dividing by the unbalance eccentricity e_u. The speed ω is made dimensionless by dividing by the rotor critical speed on rigid supports ω_{cr}. The rotor synchronous response was calculated for various combinations of unbalance and disk skew. Note that for this rotor system, there is only one critical speed which is approximately 60 percent of the rigid support value. This reduction from the rigid value is due to the flexibility of the bearings. In Cases 1–5, the values of unbalance and disk skew correspond to those originally used by Benson. This was done in order to verify the accuracy of the matrix transfer procedure.

Fig. 2 illustrates the disk amplitude versus speed for various cases of disk unbalance and skew. With unbalance only, it is seen that the disk peak amplitude is 9.5. When the rotor is operating well above the critical speed, the dimensionless amplitude is 1. Therefore, the rotor has an amplification factor of 9.5 at the critical speed.

Fig. 3 represents the disk phase angle change versus speed for the various cases of disk skew and unbalance. For the case of unbalance alone, the rotor experiences a 90 deg phase shift at the critical speed. Above the critical, this phase angle increases to 180 deg and then remains constant for speed ratios in excess of $f = 1$. This phase angle behavior corresponds to the phase angle response of the single mass Jeffcott model.

In Cases 2 and 3, positive and negative disk skew only are considered. For the amount of disk skew assumed, Fig. 2 shows that the amplitude at the critical speed is approximately 2. Above the critical speed, the amplitude will decrease with increasing speed. This physically corresponds to the situation in which the disk is straightening out and is attempting to rotate about its principal inertia axis. For the case of radial unbalance only, at super critical speeds, the disk will rotate about its mass center. This will cause a circular orbit or radius e_u, which represents the displacement of the mass center from the shaft elastic axis.

For the case of disk skew only, Fig. 3 shows that the disk phase angle will change through 90 deg at the critical speed and on to approximately 180 deg for $f = 1.0$. For the case of negative disk skew, the phase angle change observed at the disk is almost identical to the response observed with radial unbalance. For positive disk skew, the phase angle changes are 180 deg out of phase with the negative disk skew phase angles and vary from 180 deg to approximately 360 deg. One slight variation in the phase angle behavior, in comparison to the response with pure unbalance, is the phase behavior at supercritical speeds in which $f > 1$. Here it is seen that the Case 2 phase angle reduces slightly from 180 to 150 deg for f varying from 1 to 5. It will be seen later that the observation of the phase change on the rotor at supercritical speeds is an indicator that disk skew is present in the system.

In Case 4, a combination of unbalance and negative disk skew is assumed. In this situation, the unbalance moment acts in conjunction with the radial unbalance to increase the rotor shaft motion at the disk location. The response of Case 4 is equivalent to a linear vector superposition of Cases 1 and 2. Since Fig. 3 shows that the phase angle change for radial unbalance and negative disk skew is similar, the vector combination of positive unbalance and negative disk skew will always result in an increase in rotor response. This can be observed in Fig. 2, Case 4, where the amplitude at the critical is 11.5. For Case 5, unbalance and a positive disk skew are assumed. In this situation, the maximum amplitude at the critical speed has reduced to 7.5. Note that by shifting the disk skew by 180 deg, the rotor amplitude has been decreased from 11.5 to 7.5.

In the analytic equations of motion developed by Benson or in the matrix transfer equations of motion, the system is assumed to be linear. Therefore, the principle of linear superposition of loads may be applied. It will be shown later, that if the unbalance in this case were reduced by a factor of 4.75, then the combination of unbalance and positive disk skew would result in zero amplitude at the critical speed. This observation was not originally made in the Benson analysis.

If one were to observe the amplitude of an overhung disk with a combination of unbalance and disk skew, Fig. 2 shows that the unbalance response looks very similar to the standard response as obtained for the single mass Jeffcott rotor. That is, the amplitude reaches a peak and then reduces to a constant value. Fig. 3 shows that the phase angle changes observed at the disk for various combinations of both unbalance and disk skew are also very similar in appearance to the standard single mass Jeffcott model without gyroscopic effects. Hence, it is not readily apparent from the observation of the disk unbalance response and phase angle that there may be disk skew present in the system. For the speed range from 1 to 5, there is a slight reduction in the phase angle for the case of disk skew alone. Since this phase angle change in quite small, it would be difficult to determine the amount of disk skew present in the system by observation of the phase angle change at the disk end. The best way to determine if a system has disk skew is to observe the motion at locations other than the disk. Next, it will be shown that the amplitude of motion and the phase change at the near and the far bearing locations, can be used to indicate disk skew effects. These amplitude and phase characteristics are not observed in the overhung rotor system with conventional radial unbalance only.

Fig. 4 represents the amplitude of motion for the various cases of radial unbalance and disk skew as observed at the near bearing. For

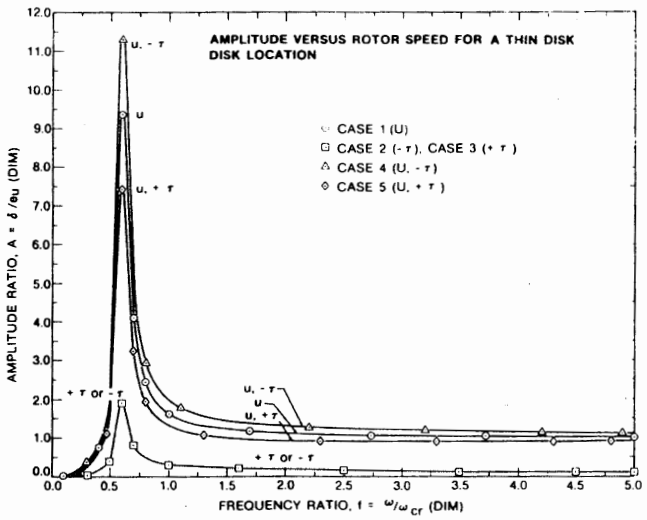

Fig. 2 Dimensionless disk amplitude versus rotor speed for a thin disk

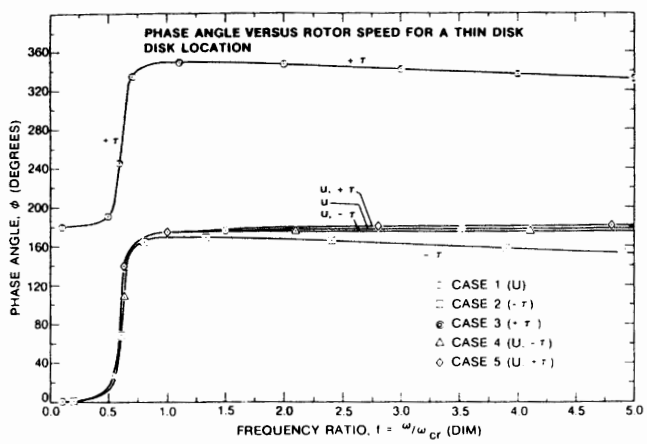

Fig. 3 Disk phase angle versus rotor speed for a thin disk

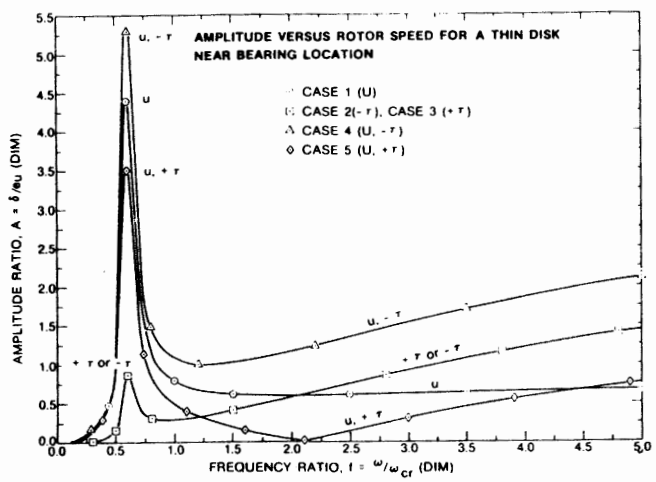

Fig. 4 Dimensionless near bearing amplitude versus rotor speed for a thin disk

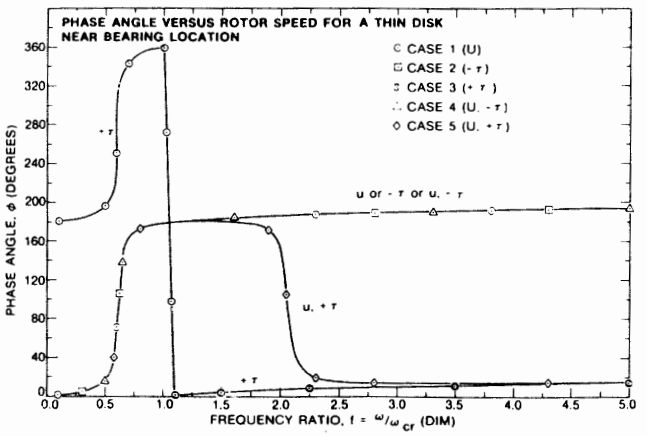

Fig. 5 Near bearing phase angle versus rotor speed for a thin disk

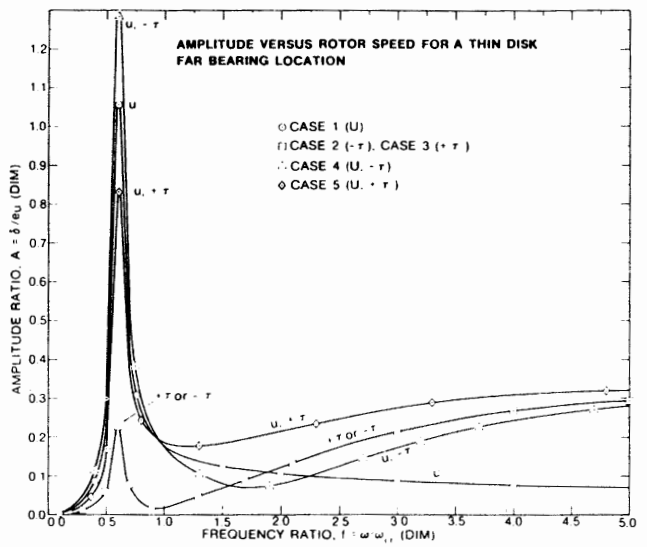

Fig. 6 Dimensionless far bearing amplitude versus rotor speed for a thin disk

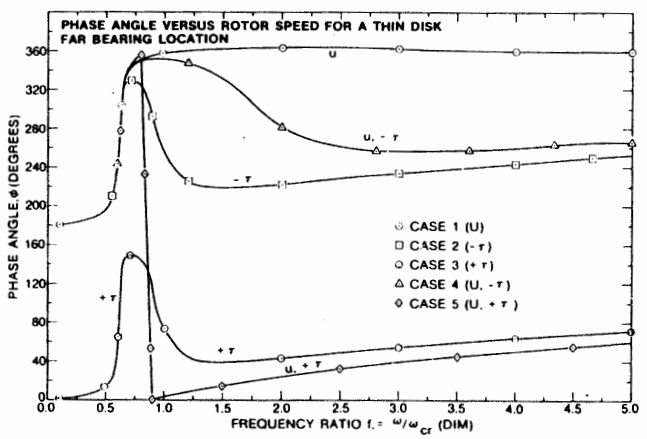

Fig. 7 Far bearing phase angle versus rotor speed for a thin disk

the case of radial unbalance only, the maximum amplitude at the near bearing is approximately one-half of the amplitude at the disk location. Upon passing through the critical speed, the dimensionless unbalance response is approximately 0.7 and remains constant with speed. The shape of the curve with unbalance at the near bearing is similar to the observed amplitude at the disk location. For the case of disk skew only, the maximum amplitude at the near bearing is 1, which again is approximately one-half of the amplitude at the disk location. Above the critical, the amplitude reduces and reaches a minimum at approximately $f = .9$. However, as the rotor speed is increased above $f = 1.0$, the rotor amplitude increases with speed.

The associated phase angle changes for the near bearing are shown in Fig. 5. The important characteristic to observe is that disk skew causes an increase in amplitude with little increase in phase angle. At first one would suspect that the rotor amplitude of motion is slowly building up due to the approach of a second critical speed. However, for this system there is no second critical speed of forward synchronous precession. The buildup in rotor amplitude is due to the skewed disk attempting to straighten out and rotate about its principal inertia axis.

Fig. 4 illustrates that the worst combination is radial unbalance and negative disk skew. This case causes a maximum amplitude of 5.3 to

occur at the near end. The minimum response at the near bearing occurs at a speed ratio of $f = 1.2$. Above this speed, the rotor amplitude continues to increase in value. However, from the phase relationship for the combination of unbalance and negative disk skew a conventional 0–180 deg phase shift is again observed.

If a positive disk skew is incorporated with the radial unbalance, there is a reduction in the amplitude of motion at the near bearing. The amplitude of motion continues to reduce and actually goes to zero at a frequency ratio of $f = 2.1$. At this speed, the near bearing is perfectly balanced. Associated with the reduction to zero amplitude is a reversal in the phase angle from 180 deg to a value approaching 15 deg. This phase angle reversal has also been observed in rotors with flexible foundations [3] and radial unbalance only. From the large phase angle shift, one might improperly conclude that the rotor is going through a housing or support resonance. However, the overhung rotor in this analysis does not have a flexible foundation. Therefore, it is disk skew that causes this unusual behavior.

Figs. 6 and 7 represent the amplitude and phase angle changes for the various conditions of unbalance and disk skew at the far end bearing. For the case of unbalance only, (Case 1), the maximum amplitude is 1.05 at the critical speed. At speeds well above the critical, the amplitude reduces to an asymptotic value of 0.07. Thus we see that for this model, radial unbalance at the disk causes a maximum displacement of 9.5 at the disk, 4.5 at the near bearing and only 1.06 at the far end bearing. The phase angle for Case 1, at the far end, varies from 180 to 360 deg with a shape that is similar to the Case 1 phase angle change observed at the disk and the near bearing. However, the far end bearing phase angle is 180 deg out of phase to the disk or near end bearing. Therefore, with unbalance alone, the amplitude response at the far bearing is only approximately 10–15 percent of the response observed at the disk and is out of phase with it.

If we examine Fig. 6 for the far end bearing with disk skew alone, the maximum amplitude is 0.22 at the critical speed, which again is only 10 percent of the value observed at the disk. However, the interesting phenomena observed in this case is that upon passing through the critical speed, the amplitude reduces and reaches a minimum at $f = .9$ and then continues to increase with speed. The examination of Fig. 7 for the phase angle change due to disk skew is even more revealing. The phase angle change through the critical is only 150 deg instead of 180 deg. After passing through the critical speed, the phase angle reduces over 100 deg from its maximum value at $f = 9.7$. Above $f = 1.5$, the phase angle gradually begins to increase.

From the data examined, it can be concluded that a rapid phase angle reversal at the far bearing, after passing through the critical speed, is indicative of a significant disk skew in the overhung rotor system. This reversal of phase angle has an important effect on the far bearing response when both unbalance and disk skew are present. At all of the rotor stations, the phase angles due to positive unbalance and negative disk skew are in-phase when passing through the critical speed. This implies that the vector addition of the two effects will result in an increase in amplitude at all stations along the rotor at the critical speed. After passing through the critical speed region, the far end phase angle with negative skew deviates from the phase angle due to unbalance alone. This then causes a reduction in amplitude at the far bearing. Another important characteristic to observe at the far end bearing is that at $f = 0.9$, the amplitudes due to unbalance alone, and in combination with disk skew, all cross over. Therefore, while the Case 5 amplitude is less than the unbalance amplitude at the critical speed, it has the highest amplitudes of all five cases at speeds above $f = 0.9$.

In all cases where disk skew is present, the far end shaft amplitude increases with speed above $f = 1.5$. This type of behavior is not observed at the disk. Therefore, in order to detect a possible condition of the disk skew in an overhung wheel, it is desirable to monitor the amplitude and phase angle behavior at both the near and the far end bearing positions. For example, with unbalance and disk skew, the near bearing amplitude of motion may increase at speeds above the critical speed without any associated phase angle change as in Case 4. At the far bearing location, the amplitude may increase at super-critical speeds with increasing or decreasing phase angles. The behavior, as shown by Figs. 6 and 7, has been observed numerous times in industry, not only with overhung rotors, but also with conventional rotors with inboard disks. The increase in amplitude above the critical speed with and without a change in phase angle has often been perplexing to investigators, particularly in the case when the operation is far removed from a second critical speed. Figs. 4–7, for the behavior of the near and the far bearings, show that disk skew can cause phase angle shifts which cannot be generated by radial unbalance alone. The reversal of phase angle change at the far bearing after passing through the first critical speed, and the increase in amplitude, is an indication of a skewed disk or a moment unbalance distribution acting at the opposite end of the machine. Notice that this phase reversal is not observed at the disk, itself.

Balancing the Overhung Thin Disk Rotor

From the behavior of the single mass overhung rotor with unbalance and disk skew, it is observed that the characteristic bearing amplitudes and phase angles significantly differ from those of the conventional single mass Jeffcott model. It is then desirable to consider various techniques to balance the overhung rotor configuration with a skewed disk. The previously discussed case of positive disk skew only ($\tau = +0.0684$ deg) was selected as the rotor excitation to be balanced out. No radial unbalance is assumed. Figs. 8–10 are the balancing plots of amplitude versus rotor speed for the far bearing, near bearing, and disk, respectively, for the various balancing cases considered.

Balance No. 1—Single Plane Disk Correction at the Critical Speed. Fig. 2, for the disk motion with various combinations of disk skew and radial unbalance, showed that the combination of positive disk skew with positive radial unbalance caused a net reduction in amplitude over the case with only unbalance. It is therefore logical to assume that if disk skew is initially present in the wheel without radial unbalance, that a radial unbalance correction weight could be placed on the wheel to cancel, or balance-out, the disk motion while passing through critical speed.

The first balance was intended to balance out the amplitude due to disk skew ($\tau = +0.0684$) using a single plane correction on the overhung disk by taking amplitude and phase measurements at the far bearing location. The balancing speed is the first critical speed ($f = 0.6$). The disk correction is determined by linear superposition using the amplitude and phase readings from the far bearing probe (Figs. 6, 7) due to the assumed unbalance from Case 1 and positive disk skew from Case 3. The dimensionless amplitude responses at the far bearing due to unbalance and disk skew are: A_F = total far bearing amplitude; A_{Fu} = far beairng amplitude due to unbalance at the disk = 1.059 L 270 deg; A_{F_τ} = far bearing amplitude due to positive disk skew = 0.225 L 90 deg; U = Case 1 unbalance at disk = 8114.53 L 0 deg gm-cm (112.66 L 0 deg oz-in) and; U_B = unbalance correction at disk.

The amplitude of motion at the far end bearing is a linear superposition of the influences of disk skew and unbalance as follows:

$$A_F = \left(\frac{A_{Fu}}{U} * U_B\right) + A_{F_\tau}$$

$$= \frac{1.059 \text{ L } 270 \text{ deg}}{8114.53 \text{ L } 0 \text{ deg}} * U_B + 0.225 \text{ L } 90 \text{ deg} \quad (2)$$

Specifying that the unbalance correction weight U_B will cause the total amplitude A_F at the far end bearing to be zero. The required amount of balance correction weight is given by

$$U_B = -\frac{0.225 \text{ L } 90 \text{ deg}}{0.00013 \text{ L } 270 \text{ deg}} = \frac{1724.03 \text{ L } 0 \text{ deg gm-in}}{(23.93 \text{ L } 0 \text{ deg oz-in})}$$

With the correction, Fig. 8 indicates that the resulting far bearing amplitude at the first critical is reduced to 0.025 from the initial amplitude of 0.225. The near bearing amplitude (Fig. 9) is reduced from 0.88 to 0.05, and the disk amplitude (Fig. 10) is reduced from 1.93 to 0.11. After this balance, the rotor can safely pass through this critical without danger of excessive amplitudes at the bearings and the disk. Fig. 10 shows that by taking influence coefficients at the far bearing, when operating through the first critical speed, the disk may

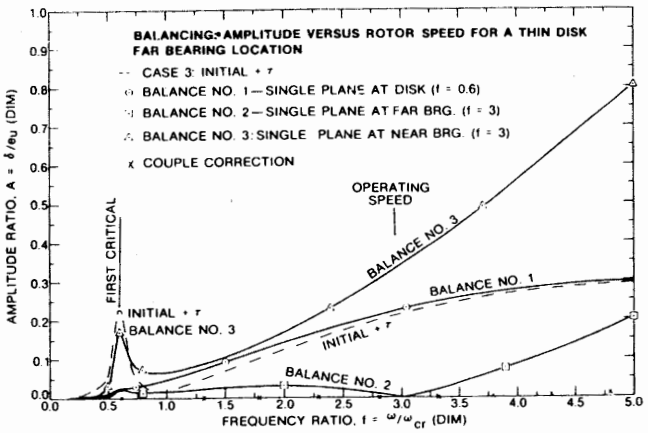

Fig. 8 Amplitude at the far bearing versus speed for various balancing cases

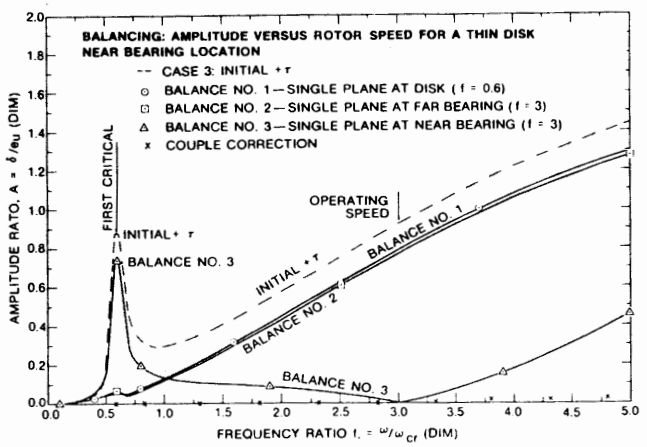

Fig. 9 Amplitude at the near bearing versus speed for various balancing cases

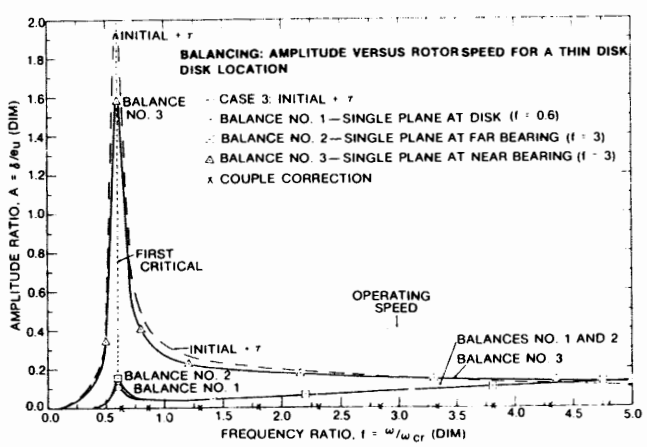

Fig. 10 Amplitude at the disk versus speed for various balancing cases

be successfully balanced. The disk amplitude then remains well behaved with low level motion throughout the entire speed range. However, Figs. 8 and 9 show that beyond the first critical speed, the amplitudes of motion at both bearings increase, with the largest amplitude occurring at the near bearing.

Balancing No. 2—Far End Correction above the Critical Speed. The second balancing correction is intended to balance out the far bearing amplitude at a post-critical speed value of $f = 3.0$ with a single plane correction at the far bearing. It will be assumed that $f = 3.0$ is the operating speed. The correction from balance No. 1 is to remain on the disk.

The balance correction is determined by the method of influence coefficients with the following equation

$$\bar{U}_u = \bar{U}_t * \frac{\bar{Z}_1}{\bar{Z}_2 - \bar{Z}_1} \tag{3}$$

where $\bar{Z}_1$ = rotor amplitude vector before the trial weight at the balancing speed = $Z_1 e^{-j\phi_1}$; $\bar{Z}_2$ = rotor amplitude vector after the trial weight at the balancing speed = $Z_2 e^{-j\phi_2}$; $\bar{U}_t$ = unbalance trial weight vector = $U_t e^{-j\phi_1}$; $\bar{U}_u$ = rotor unbalance vector = $U_u e^{-j\phi_u}$. Then the magnitude of the balance correction is

$$|U_c| = |U_u| \tag{4}$$

and the correction phase angle is then 180 deg out of phase with the unbalance. Thus

$$\phi_c = \phi_u + 180 \text{ deg} \tag{5}$$

For balance No. 2 at the far bearing for $f = 3.0$ the balancing information is: $\bar{Z}_1 = 0.2264\, e^{-j50.35\text{deg}}$ dim; $\bar{U}_t = 720.27\, e^{-j129.65\text{deg}}$ gm-cm ($10\, e^{-j129.65\text{deg}}$ oz-in); $\bar{Z}_2 = 0.53868\, e^{-j142.53\text{deg}}$ dim.

The resultant balance correction is $\bar{U}_c = 275.37\, e^{-j195.0118\text{deg}}$ gm-cm ($3.8232\, e^{-j195.0118\text{deg}}$ oz-in). Balance No. 2 was successful in reducing the far bearing amplitude (Fig. 8) from 0.2264 to 0.0 at $f = 3.0$, without disturbing the first balance at $f = 0.6$. The near bearing and disk amplitude remained unchanged as indicated in Figs. 9 and 10, respectively.

Balance No. 3—Near Bearing Correction above the Critical Speed. The third balance is intended to reduce the near bearing amplitude (Fig. 9) at operating speed ($f = 3.0$) without disturbing the previous two balance improvements. The balancing information is: $\bar{Z}_1 = 0.7716\, e^{-j9.507\text{deg}}$ dim; $\bar{U}_t = 720.27\, e^{-j190\text{deg}}$ gm-cm ($10\, e^{-j190\text{deg}}$ oz-in.); and $\bar{Z}_2\, 0.59723\, e^{-j5.806\text{deg}}$ dim.

The resultant correction is then $\bar{U}_c = 3091.15\, e^{-j177.6197\text{deg}}$ gm-cm ($42.9167\, e^{-j177.6197\text{deg}}$ oz-in.).

Balance No. 3 was successful in reducing the near bearing amplitude (Fig. 9) from 0.7716 to 0.0 at $f = 3.0$. However, the amplitude at the first critical ($f = 0.6$) significantly increased from 0.06 to 0.735. The other two rotor locations also show detrimental results. At the far bearing (Fig. 8) the amplitude increased from 0.02 to 0.17 at the first critical, and from 0.0 to 0.34 at the operating speed. In fact, at speeds above the first critical, the far bearing amplitudes are worse than the original response caused by the skewed disk (Case 3) before balancing. The amplitudes at the disk (Fig. 10) indicate an increase from 0.14 to 1.58 at the first critical. At operating speed, the amplitudes are the same as for the initial rotor before balancing.

From these three balancing runs, it is evident that while the single plane balancing technique is sufficient for balancing out the amplitudes for a specific rotor location and speed, it is not successful in balancing the overall overhung rotor over the operating speed range. It is then desirable to try balancing with a couple correction.

Balancing with a Couple Correction

A couple correction consists of two correction weights separated by the thickness of the disk and 180 deg out of phase with each other. This produces an equivalent balance moment vector, whereas the single plane corrections produce equivalent balance force vectors.

Starting with the original rotor with positive disk skew only (Case 3), a trial couple is applied to the disk to balance the rotor at the first critical ($f = 0.6$). Then the influence coefficient technique (equation (3)), as previously described for single plane balancing, is used. However, the trial weight vector becomes a trial couple vector. The balancing information is: $\bar{Z}_1 = 1.9312\, e^{-j245.66\text{deg}}$ dim; $\bar{U}_t = 720.27\, e^{-j0\text{deg}}$ gm-cm ($10\, e^{-j0\text{deg}}$ oz-in couple); and $\bar{Z}_2 = 1.9028\, e^{-j245.66\text{deg}}$ dim.

The resulting couple balance correction vector is then

$$\bar{U}_c = 48978.15 e^{-j0\text{deg}} \text{ gm-cm } (680\, e^{-j0\text{deg}} \text{ oz-in. couple})$$

With this correction, Figs. 8–10 indicate essentially zero amplitudes for all three rotor locations throughout the speed range.

There are numerous rules of thumb for estimating reasonable amounts of residual unbalance for analytical rotor response analyses. However, it is often difficult for a designer to physically arrive at

reasonable values of the disk skew angle. For small disk skew angles, it can be shown that two balance correction weights placed on a disk 180 deg out of phase and separated by distance w is equivalent to a uniform disk skewed an angle τ from the vertical.

The transformation angle to principal directions for a disk with a couple unbalance is given by

$$\tan 2\theta_p = \frac{2I_{12}}{I_{11} - I_{22}} \tag{6}$$

The product of inertia term is given by

$$I_{12} = \int_v \rho x Z dm = \frac{Uw}{\text{Kg}} \tag{7}$$

For small disk angles

$$\theta_p = \tau = \frac{Uw}{K(I_p - I_t)} \tag{8}$$

Where τ = disk skew angle (radians); U = equivalent unbalance couple, gm-cm (oz-in); w = disk thickness, cm (in.); I_p = disk polar weight moment of inertia, N-cm^2 (lb-in.^{2}); I_t = disk transverse weight moment of inertia, N-cm^2 (lb-in^2); and K = constant = 102 gm/N (= 16 oz/lb).

As an example, the equation (8) was applied to the overhung rotor discussed in this paper. The known parameters are $I_p = 4.082 \times 10^6$ N-cm^2 (1.422×10^5 lb-in^2); $I_t = 2.039 \times 10^6$ N-cm^2 (7.106×10^4 lb-in^2); $w = 5.08$ cm (2.0 in.); and $\tau = 1.194 \times 10^{-3}$ rad (0.0684 deg).

The equivalent unbalance couple can then be calculated from equation (8)

$$U = \tau K(I_p - I_t)/w = 4.8979 \times 10^4 \text{ gm-cm (679.9 oz-in.)}$$

This is the same answer as was found by the influence coefficient method with the trial couple.

Summary

The sample problem of the overhung rotor with disk skew illustrates the influence of disk skew on unbalance response and phase angle changes. It produces an effect which cannot be obtained with the usual unbalance distribution on a flexible rotor. This effect is the occurrence of a rapid reduction in phase angle at the far bearing upon passing through the critical speed. The sample problem also shows that it is impossible to balance the rotor at all speeds with single plane radial unbalance corrections in the presence of a skewed disk. The equations of motion to include disk skew or shaft bow may be expressed in matrix transformation form or by a modal formulation as has been done by Childs [14] or Gunter and Choy [15]. A condition for modal balancing a particular critical speed can be obtained from [15] by setting the modal forcing function P_{xi} for the i-th mode equal to zero. This results in the condition

$$\phi_{ij}{}^t m_j e_{uj}[\omega^2 \cos(\omega t + \alpha_j) + \dot{\omega} \sin(\omega t + \alpha_j)] + \phi_{ij}{}'^t \tau_j (I_p - I_t)_j [\omega^2 \cos(\omega t + \beta_j) + \dot{\omega} \sin(\omega t + \beta_j)] = 0 \tag{9}$$

Where ϕ_i = i-th mode shape and ϕ_i' = i-th mode shape slope. From the above condition, it is apparent that if the unbalance is selected to balance out one critical speed due to the presence of disk skew, the system will not be balanced at high critical speeds.

Conclusions—Thin Disk Overhung Rotor

1 A skewed disk will excite the first critical speed of an overhung rotor.

2 A radial disk correction can always be selected to balance out the effect of disk skew at the first critical speed.

3 Although the rotor balance may be acceptable at the first critical speed, the bearing forces and rotor amplitudes may be unacceptable at higher speeds. This system cannot be adequately balanced by single plane procedures.

4 Amplitudes and phase angles monitored at the overhung disk appear to be similar to the behavior of the elementary Jeffcott rotor model. Hence disk skew effects cannot be distinguished from unbalance by monitoring the motion only at the disk location.

5 The response characteristics at the bearings of the overhung rotor can differ considerably from Jeffcott behavior when disk skew is introduced. The amplitude is not constant above the first critical-instead, it increases with speed.

6 At the far bearing, a rapid decrease in phase angle above the first critical speed is an indication of significant disk skew. Hence, a probe at the far bearing end can indicate disk skew.

7 Two unbalance weights placed on a disk 180 deg out of phase and separated by an axial distance w can create an equivalent disk skew in the rotor. Hence, any grinding of impeller wheels in which the correction planes on the front and back are 180 deg out of phase can create equivalent disk skew effects.

References

1 Lund, J. W. and Orcutt, F. K., "Calculations and Experiments on the Unbalance Response of a Flexible Rotor," *Journal Engineering for Industry*, Nov. 1967.

2 Kawamo, K., Matsukura, Y., and Inoue, T., "Analysis of Lateral Vibration Characteristics of Rotating Shafts with Flexible and Axi-Asymmetric Bearings," 1975, Joint JSME-ASME Applied Mechanics Western Conference, 1975.

3 Kirk, R. G. and Gunter, E. J., "The Effect of Support Flexibility and Damping on the Synchronous Response of a Single-Mass Flexible Rotor," ASME *Journal of Engineering for Industry*, Vol. 94, No. 1, Feb. 1972, pp. 221–232.

4 Wolfe, W. A. and Wong, P. Y., "On the Transfer Matrix for Rotor Dynamics," Manuscript No. 72-CSME-37, EIC Accession No. 1320, July 3, 1974.

5 Barrett, L. E., Gunter, E. J., Allaire, P. E., "Optimum Bearing and Support Damping for Unbalance Response and Stability of Rotating Machinery," ASME JOURNAL ENGINEERING FOR POWER, Dec. 1976.

6 Koenig, E. C., "Analysis for Calculating Lateral Vibration Characteristics of Rotating Systems with Any Number of Flexible Supports, Part 1—The Method of Analysis," *Journal Appl. Math.*, Dec. 1961.

7 Kikuchi, K., "Analysis of Unbalance Vibration of Rotating Shaft System with Many Bearings and Disks," *JSME Bulletin*, June 16, 1969.

8 Salamone, D. J., *Synchronous Unbalance Response of a Multimass Flexible Rotor Considering Shaft Warp and Disk Skew*, M.S. Thesis, University of Virginia, May 1977.

9 Nicholas, J. C., Gunter, E. J., and Allaire, P. E., "Effect of Residual Shaft Bow on Unbalance Response and Balancing of a Single Mass Flexible Rotor," Parts I and II. ASME JOURNAL OF ENGINEERING FOR POWER, Vol. 98, Series A, No. 2, April 1976, pp. 171–189.

10 Lund, J. W., "Rotor-Bearing Dynamics Design Technology, Part V: Computer Program Manual for Rotor Response and Stability," Air Force Technical Report AFAPL-TR-65-45, Part V, May 1965.

11 Yamamoto, T., "On the Critical Speeds of a Shaft," *Memoirs of the Faculty of Engineering*, Nagoya University, Japan, Nov. 1954.

12 Benson, R. C., *Dynamic Response of an Overhung, Unbalance Skewed Rotor in Fluid Film Bearings*, M.S. Thesis, University of Virginia, Aug. 17, 1974.

13 Salamone, D. J. and Gunter, E. J., "Effects of Shaft Warp and Disk Skew on the Synchronous Unbalance Response of a Multimass Rotor in Fluid Film Bearings," *Topics in Fluid Film Bearing and Rotor Bearing System Design and Optimization*, ASME Book No. 100118, pp. 79–107, April 1978.

14 Childs, D. W., "Two Jeffcott-Based Modal Simulation Models for Flexible Rotating Equipment," ASME *Journal Engineering for Industry*, Aug. 1975.

15 Gunter, E. J., Choy, K. C., and Allaire, P. E., "Modal Analysis of Turborotors Using Planar Modes—Theory," *Journal of the Franklin Institute*, Vol. 305, No. 4, pp. 221–243, April 1978.